Automation and Machine Learning (2025)
Clausius Scientific Press, Canada

DOI: 10.23977/autml.2025.060116
ISSN 2516-5003 Vol. 6 Num. 1

Energy-Efficient Obstacle Avoidance Optimization for Multi-Vehicle Systems Based on an Improved Artificial Potential Field with PID Control

Guanghong Liang, Weigang Yan, Yongxiang Fan

School of Energy and Power Engineering, University of Shanghai for Science and Technology, Shanghai, China

Keywords: PID Control; Multi-Vehicle Systems; Formation Obstacle Avoidance; Leader–Follower Method; Artificial Potential Field; Energy Efficiency

Abstract: In multi-vehicle formation scenarios, obstacle avoidance in unknown environments presents several challenges, such as obstacles near the target, entrapment in local minima, and dynamic obstacle interference. To address these issues in multi-vehicle formation control, this paper proposes an optimization algorithm that enhances the artificial potential field (APF) method with PID control. Simulation experiments demonstrate that, compared to benchmark algorithms, the proposed method achieves reductions of 32.4%, 41.9%, 24.8%, and 32.0% in the number of total iterations, formation efficiency function value, energy consumption, and iteration standard deviation, respectively. The improved approach effectively resolves slow obstacle avoidance near the target, overcomes local minima issues, handles dynamic obstacles, exhibits enhanced robustness, and realizes energy-efficient obstacle avoidance in complex environments.

1. Introduction

Against the backdrop of global energy scarcity and environmental degradation, the automotive industry is transitioning rapidly toward new energy, intelligentization and energy-efficient development. In contrast, multi-robot systems offer a more economical, efficient, and time-saving solution, enabled by resource sharing and mass production mechanisms, which significantly reduce overall cost and enhance economic viability in practical applications. As robotic production lines become more prevalent, there has been a noticeable shift in demand from standalone robots to autonomous, collaborative multi-robot systems (Dahiya et al., 2023) [1].

Recent years have witnessed extensive research in multi-vehicle formation control (Oh et al., 2015) [2], with particular emphasis on formation establishment, maintenance, reconfiguration, obstacle avoidance, and adaptive coordination (Wang et al., 2023) [3]. However, this method exhibits a critical flaw: excessive reliance on the leader vehicle compromises system robustness due to its dominant role. As depicted in Figure 1, the conventional APF method also suffers from inherent limitations (Fan et al., 2020) [4], including: (A) Goal Non-Reachability with Nearby Obstacles (GNRON), (B) local minima entrapment, and (C) challenges in dynamic obstacle avoidance.

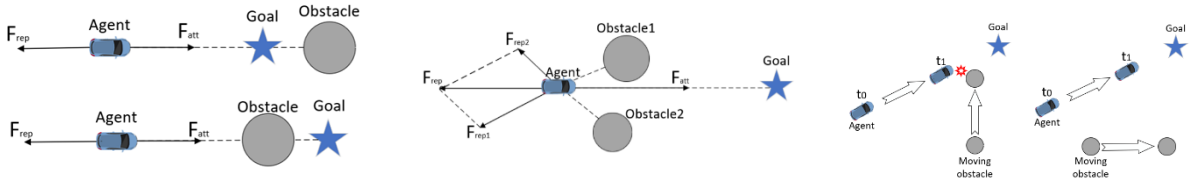

Goal not Reachable or Not Obtainable Trapped in local Minimum Reion Obstacle avoidance in dynamic environment

Figure 1: Problems of traditional algorithms

To resolve goal non-reachability with nearby obstacles (GNRON). Jia and Wang [5] eliminated GNRON by amplifying the attractive potential gradient near targets. Yang et al. [6] implemented potential field filling through supplementary fields in target regions. Sfeir et al. [7] devised an environment-agnostic repulsive potential field, while Zhang [8] redefined repulsive potentials using flow-field coordinates.

Regarding local minima entrapment, Matoui et al. [9] utilized non-minimum velocity algorithms. Sun et al. [10] employed dynamic window approaches for escape, whereas Xian-Xia et al. [11] deployed virtual obstacles near minima via sector partitioning. Li et al. [12] constructed virtual local targets through novel potential functions, and Wu et al. [13] integrated simulated annealing with deterministic annealing for minima evasion.

For dynamic environment obstacle avoidance, Montiel et al. [14] established parallel-evolution artificial potential fields. Cheng et al. [15] synthesized velocity methods with APF, while Cao et al. [16] applied limit-cycle theory to multi-vehicle systems, overcoming APF limitations. Zheng et al. [17] developed a fuzzy APF-based formation strategy, effectively resolving formation control and obstacle avoidance in dynamic scenarios.

2. Improvements Based on the Artificial Potential Field Method

In the Artificial Potential Field (APF) method (Khatib, 1985) [18], the attractive gain coefficient (k_{att}) and the repulsive gain coefficient (k_{rep}) play a crucial role in determining the effectiveness of obstacle avoidance. However, the selection of these coefficients is typically based on empirical knowledge rather than being optimized for specific environments. As a result, several issues may arise, such as the occurrence of local minima, elongated obstacle avoidance paths, and difficulties in handling dynamic environments.

2.1. Enhancement of the Attractive Potential Function

2.1.1. Long-Distance Attractive Force Adjustment

In scenarios where the map is large and the target point is distant, the attractive force is proportional to the distance to the goal.

Define the target distance difference e in equation 1:

$$e = \begin{cases} q_0 - q_g & if\ leader \\ q_i - q_e & if\ follower \end{cases} \quad (1)$$

In the proposed method: q_0 denotes the current position of the leader, and q_g represents the leader's target position; q_i refers to the current position of the follower, while q_e indicates the expected target position of the follower.

The formula for the enhanced gravitational potential field is shown as equation 2:

$$U_{att}(e) = \begin{cases} \frac{1}{2}k_{att}e^2, & e \le d \\ dk_{att}e - \frac{1}{2}k_{att}d^2, & e > d \end{cases} \quad (2)$$

Where $U_{att}(e)$ represents the gravitational potential field; k_{att} is a gravitational gain coefficient greater than 0; d is the given constant, in this case the distance factor.

The corresponding gravitational function is given in Equation. 3:

$$F_{att}(e) = -\nabla U_{att}(e) = \begin{cases} k_{att}e, & e \le d \\ -dk_{att}\frac{e}{\|e\|}, & e > d \end{cases} \quad (3)$$

2.1.2. PID-Controlled Attraction Adjustment

As the agent approaches the target position, the attractive force becomes relatively weak. the attractive potential function can be further enhanced by integrating PID control techniques.

The improved gravitational function is given in Equation 4:

$$F_{att}(e) = k_p e + k_i \int_0^t e dt + k_d \frac{de}{dt} \quad (4)$$

Where k_p, k_i and k_d represent t the proportional, integral, and derivative coefficients of the PID control, respectively. These coefficients correspond to the proportional, integral, and derivative items of the distance difference between the vehicle's current position and the target position.

The above formula represents the continuous expression of PID control, and the discrete form is expressed as shown in Equation 5:

$$F_{att}(e_i) = k_p e_i + k_i \sum_{i=1}^{N} e_i + k_d(e_i - e_{i-1}) \quad (5)$$

2.1.3. Final Form of Improved Attractive Function

Combining the two improvements of 1.1.1 and 1.1.2, the improved gravitational function is obtained as shown in Equation 6:

$$F_{att}(e_i) = \begin{cases} k_p e_i + k_i \sum_{i=1}^{N} e_i + k_d(e_i - e_{i-1}) \\ -dk_p \frac{e_i}{\|e_i\|} + k_i \sum_{i=1}^{N} e_i + k_d(e_i - e_{i-1}) \end{cases} \quad (6)$$

2.2. Enhancement of the Repulsive Potential Function

2.2.1. Spatial Repulsive Force Function Improvement

In the traditional artificial potential field (APF) method, several issues can arise—most notably, the problem of unreachable target points. To address these limitations and enhance overall performance, a modified repulsive force function is introduced.

Define obstacle distance difference s in Equation 7:

$$s = q - q_0 \tag{7}$$

Where q represents the vehicle's current position and q_0 is the obstacle's current position.

The position repulsion field function (Yang and Wang, 2013) [19] based on the distance difference between obstacles and targets is as given in Equation 8:

$$U_{repx}(s) = \begin{cases} \frac{1}{2} k_{rep} \left(\frac{1}{s} - \frac{1}{\rho_0}\right)^2 e^n, & s \le \rho_0 \\ 0, & s > \rho_0 \end{cases} \tag{8}$$

Where $U_{repx}(s)$ represents the position repulsive potential field; k_{rep} is a repulsive gain coefficient greater than 0; ρ0 is the influence distance of obstacles; n is a given constant, and 2 is taken in this paper.

The negative gradient of the position repulsion field function can be obtained, and the improved position repulsion function can be obtained as shown in Equation. 9:

$$F_{repx}(s) = -\nabla U_{repx}(s) = \begin{cases} F_{rep1} + F_{rep2}, & s \le \rho \\ 0, & s > \rho_0 \end{cases} \tag{9}$$

Among them, Frep1 and Frep2 are:

$$F_{rep1} = k_{rep}(\frac{1}{s} - \frac{1}{\rho_0})\frac{e^n}{s^2} \tag{10}$$

$$F_{rep2} = \frac{2}{n} k_{rep}(\frac{1}{s} - \frac{1}{\rho_0})^2 e^{n-1} \tag{11}$$

2.2.2. Velocity-Based Repulsive Force Improvement

The potential field function of the velocity repulsion (Cui and Song, 2018) [20] is defined as given in Equation 12:

$$U_{repv}(s_i) = \begin{cases} \frac{1}{2} k_v (s_i - s_{i-1})^2, s_i \le \rho_0 \cap \alpha \in (-\frac{\pi}{2}, \frac{\pi}{2}) \\ 0, \ else \end{cases} \tag{12}$$

Where $U_{repv}(s_i)$ represents the velocity repulsive potential field; k_v is a velocity gain coefficient greater than 0; the difference between two iterations of si represents the relative velocity between the vehicle and the obstacle; α is the angle between relative velocity and relative position.

The velocity repulsion function is given in Equation 13:

$$F_{repv}(s_i) = U_{repv}(s_i) = \begin{cases} \frac{1}{2} k_v (s_i - s_{i-1})^2, s_i \le \rho_0 \cap \alpha \in (-\frac{\pi}{2}, \frac{\pi}{2}) \\ 0, \ else \end{cases} \tag{13}$$

2.2.3. Combined Repulsive Force Function

Combine the two improvements of 1.2.1 and 1.2.2, the improved repulsion function is obtained as shown in Equation 14:

$$F_{rep}(s_i) = \begin{cases} F_{repx}(s_i) + F_{repv}(s_i), s_i \le \rho_0 \cap \alpha \in (-\frac{\pi}{2}, \frac{\pi}{2}) \\ F_{repx}(s_i), s_i \le \rho_0 \cap \alpha \notin (-\frac{\pi}{2}, \frac{\pi}{2}) \\ 0, s_i > \rho_0 \end{cases} \quad (14)$$

3. Implementation of the Multi-Vehicle Formation Obstacle Avoidance Algorithm

3.1. Control Framework

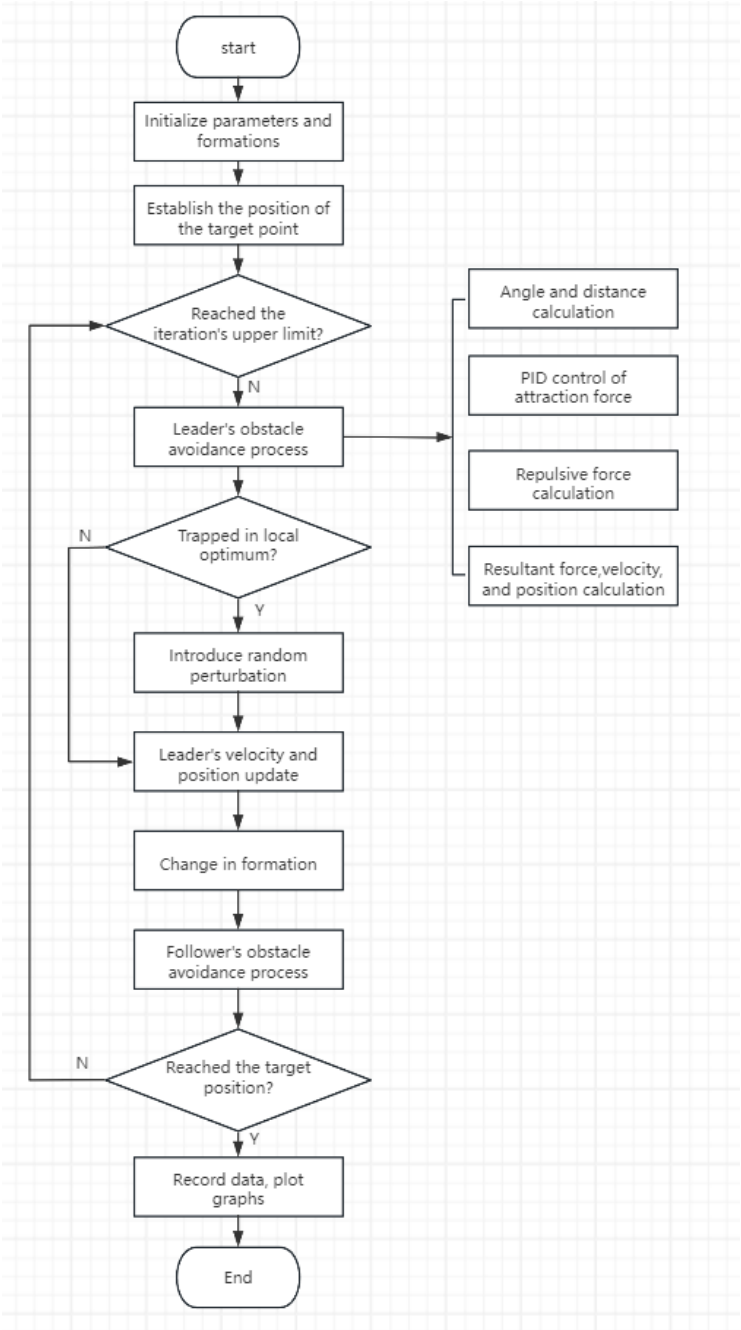

Figure 2: Multi-vehicle formation obstacle avoidance process.

A modularized multi-vehicle formation obstacle avoidance algorithm based on an improved artificial potential field method was implemented in MATLAB to enhance system scalability; as illustrated in Figure 2, its workflow involves initializing parameters and forming the initial formation, calculating gravitational forces toward the target and repulsive forces from obstacles (with boundary extraction and potential merging), iteratively computing obstacle avoidance for the leader including angle/distance calculations, PID-controlled gravitational forces, position/velocity repulsive forces, resultant force integration, local optimum detection and random perturbation if trapped, adjusting the formation upon the leader's arrival at the next waypoint to derive followers' desired positions, and having followers replicate the leader's avoidance process with additional inter-vehicle repulsion calculations to prevent collisions.

3.2. Evaluation Metrics

This study employs three established evaluation metrics: the total formation obstacle avoidance iterations, the formation efficiency function, and the standard deviation of avoidance iterations. The first two metrics evaluate algorithm performance in specified obstacle environments, while the third assesses robustness in multi-obstacle scenarios.

The formation efficiency function quantifies formation deformation during avoidance procedures—reduced deformation signifies superior performance as established by Zhang et al. [2019] [21]. Corresponding mathematical expressions are provided in Equation 15 and 16.

$$f_2 = \sum_{n=1}^{N} ((\sum_{i=1}^{l} e)/I)/N \quad (15)$$

$$N = J/m \quad (16)$$

Here, i represents the index of each follower, and e indicates the deviation of the follower's actual position from the expected position. I correspond to the total number of iterations in the formation obstacle avoidance process. To reduce computational complexity, this study uses a predetermined constant iteration interval m, set to 10. Sampling data at this interval can significantly alleviate the computational burden.

The evaluation function f3 aims to reflect the energy consumption of the car during the obstacle avoidance process. The expression for the evaluation function f_3 is shown in Equation 17:

$$f_3 = E_{oc} + E_{ic} = k_{oc} \cdot J + k_{ic} \cdot s \quad (17)$$

Here, E_{oc} denotes operational energy consumption and E_{ic} represents idle energy consumption, which are respectively related to the number of iterations J and obstacle avoidance distance s. k_{oc} and k_{ic} are their correlation coefficients, with specific values determined based on the relevant environment.

However, in complex multi-obstacle environments, the aforementioned efficiency metrics may inadequately capture the algorithm's adaptability. Therefore, the standard deviation of iteration counts during formation obstacle avoidance is introduced as an additional evaluation function to assess algorithmic effectiveness and robustness (Yanbin et al., 2018) [22], where a smaller standard deviation indicates superior performance. The calculation is defined in Equation 18 and 19:

$$f_4 = \sqrt{\sum_{k=1}^{K} (J_k - J)^2 / K} \quad (18)$$

$$J = (\sum_{k=1}^{K} J_k)/K \quad (19)$$

Where k represents the number of simulation experiments, whereas J_k represents the total iteration count for the formation obstacle avoidance in the kth simulation.

4. Simulation Experiments and Analysis

4.1. Obstacle Avoidance under Preset Conditions

In Scenario 1, three obstacle configurations were tested. In the first, an obstacle was collinear with the start and target points. as shown in Figure 3, the traditional APF method failed to complete obstacle avoidance for the three specific obstacle configurations. Although the improved IAPF method achieved partial avoidance, it still failed to reach the target within the maximum number of iterations (J = 500). In contrast, after incorporating PID control, the agents successfully reached the target under all three working conditions with iteration counts of J = 343, 381, and 351, respectively.

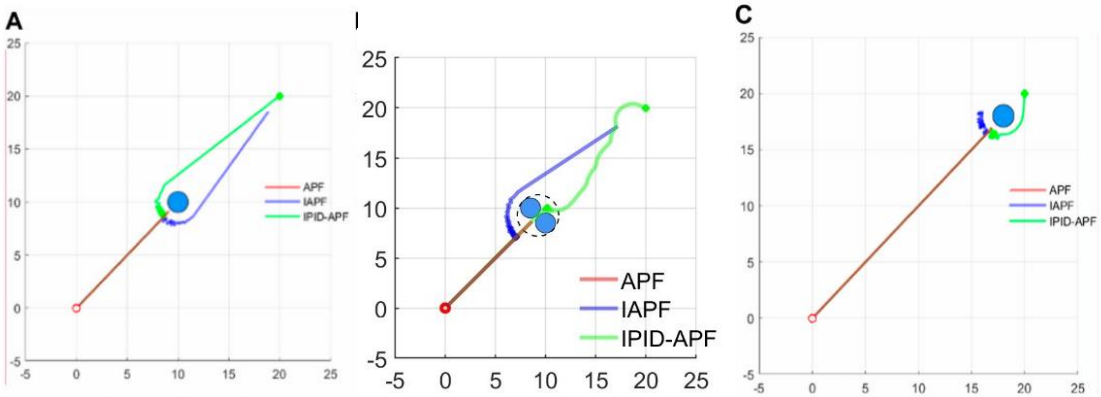

Operation 1 Path Operation 2 Path Operation 3 Path

Figure 3: Comparison of movement paths under different operating conditions

4.2. Obstacle Avoidance in Random Environments

Experiment 2 evaluates efficiency variations before and after PID control integration, addressing traditional methods' limitations in complex environments. A five-vehicle V-shaped formation (Vehicle 1 leader, Vehicles 2-5 followers) examines parameter adjustment impacts on obstacle avoidance performance. PID control refines residual parameters under configured conditions, with algorithmic performance variations observed across three randomized environments.

Environment 1:

The comparative experimental data shows that compared with the improved method, the proposed algorithm reduces the formation obstacle avoidance iterations (f_1) from 760 to 521, increasing the obstacle avoidance speed by 31.4% for faster mission completion; the formation efficiency function value (f_2) decreases from 15.9 to 5.9 (a 62.9% reduction), allowing passage through obstacle areas with a tighter formation; and the energy consumption function value (f_3) drops significantly from 351.8 to 251.5 (a 28.5% decrease). as shown in Figure 4.

Environment 2:

Building upon Environment 1's obstacle configuration, Environment 2 increased the number of obstacles from 10 to 15 to further explore the impact of introducing improved PID control on algorithm performance in more complex obstacle scenarios.

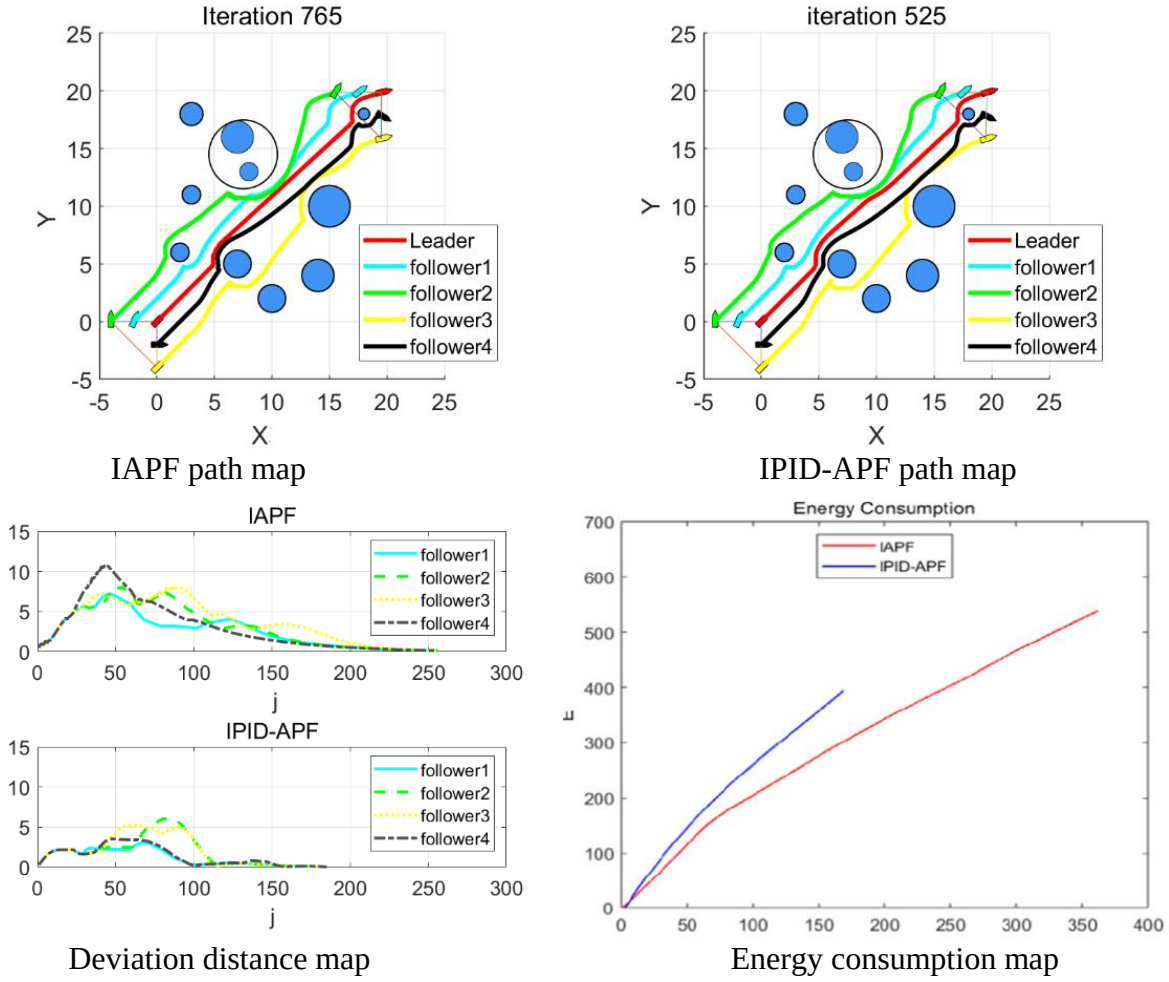

Figure 4: Environment 1 maps

Table 1: Setting parameters and corresponding function values in environment

Method	K_p	K_i	K_d	$k_{p,}$	k_i	k_d	f_1	f_2	f_3
IAPF	2	none	none	5	none	none	765	15.9	351.8
IPID-APF	4.5	1	0.025	14	1	0.03	525	5.9	251.5

Analysis of the data in Table 1 reveals that compared to the improved method, the proposed approach reduced the number of iterations (f_1) from 850 to 551 (a 35.1% reduction), lowered the formation efficiency function value (f_2) from 16 to 8.4 (a 47.5% decrease), and decreased the energy consumption function value (f_3) from 423.9 to 380.8 (a significant 10.2% drop). In Environment 3, where obstacle complexity was further increased, changes in evaluation function values were less pronounced compared to Environment 2. Nevertheless, all evaluation function values (f1, f2, f3) decreased significantly, indicating that the proposed method performs well in more complex obstacle environments and improves obstacle avoidance efficiency.as shown in Figure 5.

Table 2: Setting parameters and corresponding function values in environment

Method	K_p	K_i	K_d	$k_{p,}$	k_i	k_d	f_1	f_2	f_3
IAPF	2	none	none	5	none	none	850	16.0	423.9
IPID-APF	4.5	1	0.025	14	1	0.03	549	8.4	380.8

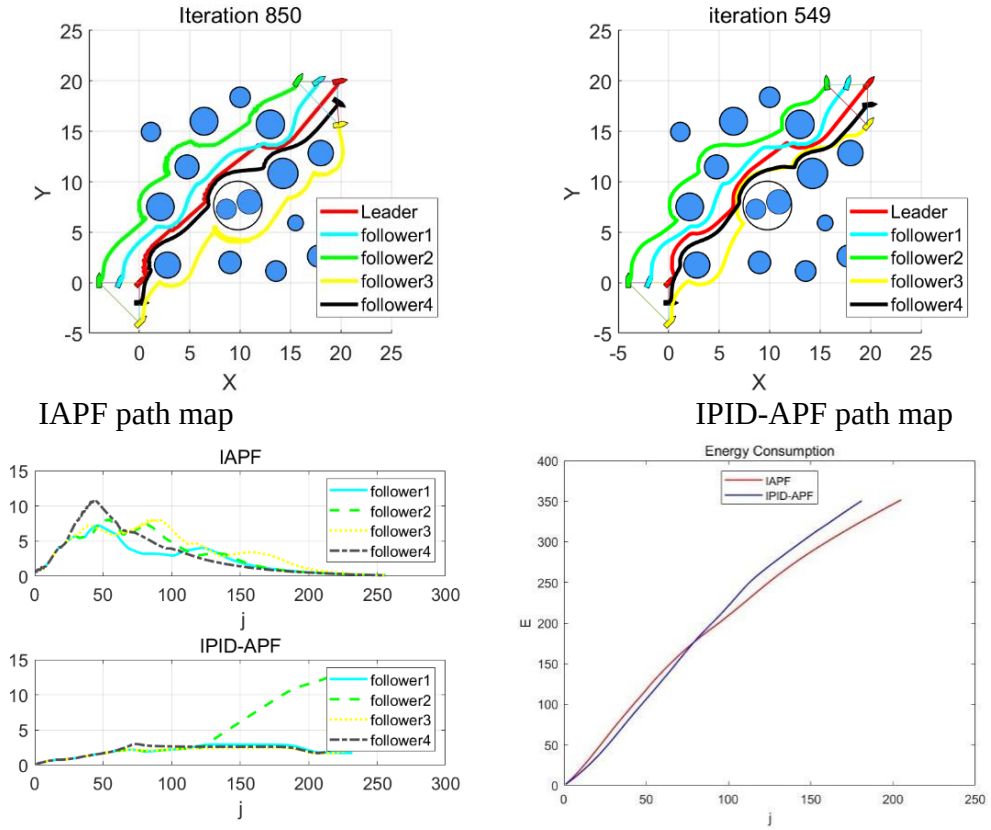

Figure 5: Environment 2 maps

4.3. 100 Trials in Random Obstacle Environments

To further verify the adaptability of the multi-vehicle formation obstacle avoidance method in random obstacle environments, after analysing two random scenarios in Experiment 2, Experiment 3 conducted 100 trials to observe the changes in efficiency function values f_1 and f_2, thereby validating the reliability of the proposed method.

The comparison of the variation curves of function values f1 and f2 of the improved algorithm in 100 experiments is shown in the Figure 6:

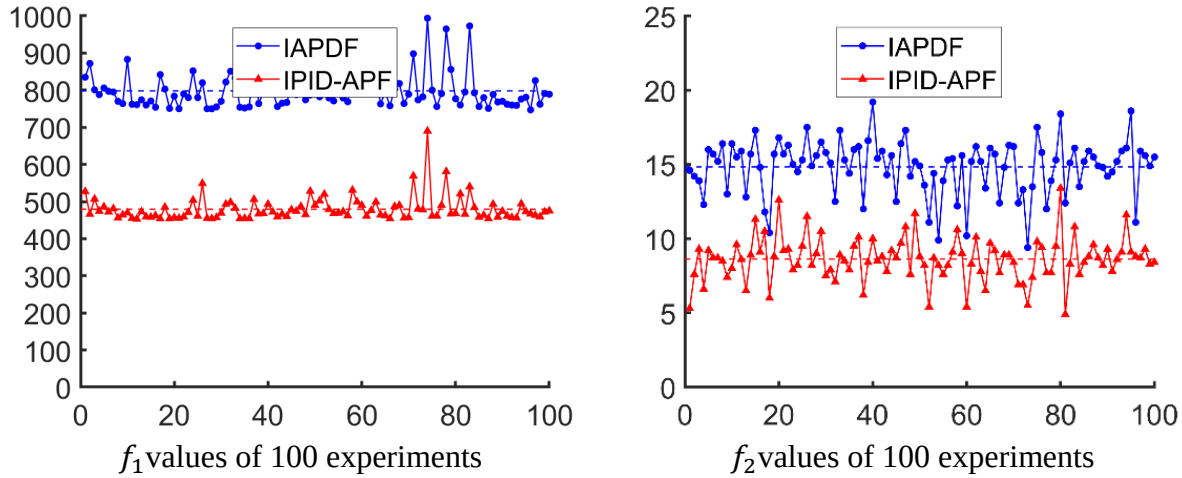

Figure 6: Comparison of efficiency functions in random environment

Table 3: Setting parameters and corresponding function values in environment

Method	f_1	f_2	f_3	f_4
IAPF	525.4	14.83	423.9	51.88
IPID-APF	850.1	8.63	318.1	35.30

4.4. Discussion

This paper conducted three groups of simulation experiments to comprehensively compare the performance of the traditional algorithm (APF), the improved algorithm (IAPF), and the proposed algorithm (IPID-APF) under various obstacle environments.

Experiment 1 involved three specific obstacle scenarios and aimed to reveal the limitations of the traditional method. As shown in Figure 6, the traditional algorithm clearly failed to accomplish the obstacle avoidance task.

As illustrated by the comparison plots In Figures 4–6 and the data analyses in Tables 1–3, the proposed algorithm outperformed others in most cases. The superior performance is reflected in the number of iterations, the degree of formation maintenance, and efficiency function values. These results highlight the importance of incorporating PID control to enhance algorithm performance.

5. Conclusions

This paper proposes a multi-vehicle formation obstacle avoidance algorithm that integrates PID control with an improved Artificial Potential Field (APF) method. By incorporating PID control into the potential field function calculation, the proposed method effectively addresses common issues such as unreachable targets, local minima, and obstacle navigation in dynamic environments.

Simulation experiments were conducted across various randomly generated obstacle scenarios, comparing the proposed algorithm with both traditional and improved APF methods. Four commonly used evaluation metrics—total number of iterations, formation efficiency, energy consumption, and iteration standard deviation—were employed to assess performance. The results show that the proposed algorithm outperforms the alternatives, achieving improvements of 32.4%, 41.9%, 24.8%, and 32.0% in the respective evaluation functions.

Therefore, the proposed approach provides an effective solution to the challenges of formation control and obstacle avoidance in complex environments involving multiple autonomous vehicles.

References

[1] Dahiya, A., Aroyo, A. M., Dautenhahn, K., and Smith, S. L. (2023). A survey of multi-agent Human–Robot Interaction systems. Robotics Aut. Syst. 161, 104335. doi:10.1016/j. robot.2022.104335

[2] Cheng, C., Zhu, D., Sun, B., Chu, Z., Nie, J., and Zhang, S. (2015). "Path planning for autonomous underwater vehicle based on artificial potential field and velocity synthesis," in 2015 IEEE 28th Canadian Conference on Electrical and Computer Engineering (CCECE), Halifax, NS, Canada (IEEE), 717–721. doi:10.1109/CCECE. 2015.7129363

[3] Wang, L., Zhu, D., Pang, W., and Zhang, Y. (2023). A survey of underwater search for multi-target using Multi-AUV: task allocation, path planning, and formation control. Ocean. Eng. 278, 114393. doi:10.1016/j.oceaneng.2023.114393

[4] Fan, X., Guo, Y., Liu, H., Wei, B., and Lyu, W. (2020). Improved artificial potential field method applied for AUV path planning. Math. Problems Eng. 2020, 1–21. doi:10. 1155/2020/6523158

[5] Jia, Q., and Wang, X. (2010). "An improved potential field method for path planning," in 2010 Chinese Control and Decision Conference, Xuzhou, China (IEEE), 2265–2270. doi:10.1109/CCDC.2010.5498836

[6] Yang, X., Yang, W., Zhang, H., Chang, H., Chen, C.-Y., and Zhang, S. (2016). "Anew method for robot path planning based artificial potential field," in 2016 IEEE 11th Conference on Industrial Electronics and Applications (ICIEA), Hefei, China (IEEE), 1294–1299. doi:10.1109/ICIEA.2016.76037841294–1299. doi:10.1109/ICIEA.2016.7603784

[7] Sfeif, J., Saad, M., and Saliah-Hassane, H. (2011). "An improved Artificial Potential Field approach to real-time mobile robot path planning in an unknown environment," in 2011 IEEE International Symposium on Robotic and Sensors

Environments (ROSE), Montreal, QC, Canada (IEEE), 208–213. doi:10.1109/ROSE.2011.6058518
[8] Zhang, C. (2018). Path planning for robot based on chaotic artificial potential field method. IOP Conf. Ser. Mater. Sci. Eng. 317, 012056. doi:10.1088/1757-899X/317/1/ 012056
[9] Matoui, F., Boussaid, B., and Abdelkrim, M. N. (2019). Distributed path planning of a multi-robot system based on the neighborhood artificial potential field approach. SIMULATION 95, 637–657. doi:10.1177/0037549718785440
[10] Sun, J., Liu, G., Tian, G., and Zhang, J. (2019). Smart obstacle avoidance using a danger index for a dynamic environment. Appl. Sci. 9, 1589. doi:10.3390/app9081589
[11] Xian-Xia, L., Chao-Ying, L., Xue-Ling, S., and Ying-Kun, Z. (2018). Research on improved artificial potential field approach in local path planning for mobile robot. Comput. Simul. Available at: http: //en. cnki. com. cn/Article_en/CJFDTotal-JSJZ201804063.htm (Accessed December 25, 2023). doi:10.3969/j.issn.1006-9348. 2018.04. 063
[12] Li, G., Yamashita, A., Asama, H., and Tamura, Y. (2012). "An efficient improved artificial potential field based regression search method for robot path planning," in 2012 IEEE International Conference on Mechatronics and Automation, Chengdu, China (IEEE), 1227–1232. doi:10.1109/ICMA.2012.6283526
[13] Wu, Z., Dai, J., Jiang, B., and Karimi, H. R. (2023). Robot path planning based on artificial potential field with deterministic annealing. ISA Trans. 138, 74–87. doi:10. 1016/j.isatra.2023.02.018
[14] Montiel, O., Sepúlveda, R., and Orozco-Rosas, U. (2015). Optimal path planning generation for mobile robots using parallel evolutionary artificial potential field. J. Intell. Robot. Syst. 79, 237–257. doi:10.1007/s10846-014-0124-8
[15] Oh, K.-K., Park, M.-C., and Ahn, H.-S. (2015). A survey of multi-agent formation control. Automatica 53, 424–440. doi:10.1016/j.automatica.2014.10.022.
[16] Cao, J. F., Ling, Z. H., Gao, C., and Yuan, Y. F. (2014). Obstacle avoidance and formation control for multi-agent based on swarming. J. Syst. Simul. Available at: http://en.cnki.com.cn/Article_en/CJFDTotal-XTFZ201403014.htm (Accessed October 17, 2023). doi:10.16182/j.cnki.joss.2014.03.040
[17] Zheng, Z., Li, Y., and Wang, Y. (2022). Research and implementation of multi-agent UAV system simulation platform based on JADE. Cham: Springer. doi:10.1007/978-3-030-99200-2_10
[18] Khatib O . Real-Time Obstacle Avoidance System for Manipulators and Mobile Robots[J]. The International Journal of Robotics Research, 1985, 5(1):90-98
[19] Yang, Y. B., and Wang, C. L. (2013). Obstacle avoidance method for mobile robots based on improved artificial potential field method and its implementation on MATLAB. J. Univ. Shanghai Sci. Technol. Available at: http://www.researchgate.net/publication/312121694_Obstacle_avoidance_method_for_mobile_robots_based_on_ improved_artificial_potential_field_method_and_its_implementation_on_MATLAB (Accessed December 25, 2023). doi:10.13255/j.cnki.jusst.2013.05.009
[20] Cui, B. X., and Song, J. R. (2018). Obstacle avoidance and dynamic target tracking of robot in unknown environment. J. Shenyang Univ. Technol. 40, 292–298. doi:10.7688/j. issn.1000-1646.2018.03.10
[21] Zhang, X., Su, W., and Chen, L. (2019). "A multi-agent formation control method based on bearing measurement," in 2019 4th International Conference on Measurement, Information and Control (New York, United States: IEEE). Available at: http://www.xueshufan.com/publication/3016828710 (Accessed December 26, 2023).
[22] Yanbin, Z., Pengxue, X. I., Linlin, W., Wenxin, F. a. N., and Mengyun, H. a. N. (2018). Obstacle avoidance method for multi-agent formation based on artificial potential field method. J. Comput. Appl. 38, 3380. doi:10.11772/j.issn.1001-9081.2018051119